CONSTRAINT ENERGIES FOR THE ADAPTATION OF 2D RIVER BORDERLINES TO AIRBORNE LASERSCANNING DATA USING SNAKES

J. Goepfert, F. Rottensteiner, C. Heipke[1], Y. Alakese, B. Rosenhahn[2]

[1]Institute of Photogrammetry and GeoInformation (IPI), Leibniz Universität Hannover
(goepfert, rottensteiner, heipke)@ipi.uni-hannover.de
[2]Institut für Informationsverarbeitung (TNT), Leibniz Universität Hannover
rosenhahn@tnt.uni-hannover.de, y_alakese@yahoo.de

Commission II

KEY WORDS: snakes, vector data, river, ALS, intensity, consistency

ABSTRACT:

The German Authoritative Topographic Cartographic Information System (ATKIS) stores the height and the 2D position of the objects in a dual system. The digital terrain model (DTM), often acquired by airborne laser scanning (ALS), supplies the height information in a regular grid, whereas 2D vector data are provided in the digital landscape model (DLM). However, an increasing number of applications, such as flood risk modelling, require the combined processing and visualization of these two data sets. Due to different kinds of acquisition, processing, and modelling discrepancies exist between the DTM and DLM and thus a simple integration may lead to semantically incorrect 3D objects. For example, rivers may flow uphill. In this paper we propose an algorithm for the adaptation of 2D river borderlines to ALS data by means of snakes. Besides the two basic energy terms of the snake, the internal and image energy, 3D object knowledge is introduced in the constraint energy in order to guarantee the semantic correctness of the rivers in a combined data set. The image energy is based on ALS intensity and height information and derived products. Additionally, features of rivers in the DTM, such as the flow direction or the river profile, are formulated as constraints in order to fulfil the semantic properties of rivers and stabilize the adaptation process. Furthermore, the known concept of twin snakes exploits the width of the river and also supports the procedure. Some results are given to show the applicability of the algorithm.

1. INTRODUCTION

1.1 Motivation

Many applications of geospatial information require a 3D representation and visualisation of the Earth's surface and the related topographic objects. In Germany the Authoritative Topographic Cartographic Information System (ATKIS®) is one of the main sources of such data. However, the relevant information is stored in a dual system that basically consists of the Digital Landscape Model (DLM) and the Digital Terrain Model (DTM). The objects in the DLM are modelled as 2D vector data, whereas the DTM represents the Earth's surface by terrain heights in a regular grid. Due to different methods of acquisition, processing, and modelling, discrepancies exist between the DLM and the DTM. This leads to semantically incorrect results if the two data sets are integrated without a geometrical adaptation. For instance, in a combined data set bodies of standing water having impossible height variations, streets with invalid height gradients, and rivers flowing uphill can be found. Therefore, the two data sets have to be suitably adapted for accurate combined visualization and processing. The Surveying Authority of the German Federal State of Schleswig-Holstein has conducted a state-wide Airborne Laser Scanning (ALS) flight for the derivation of the DTM. ALS delivers a 3D point cloud representing a Digital Surface Model (DSM) along with intensity values for each laser point. These intensities are related to the reflectance properties of the illuminated surfaces. Both the DSM and the intensities can be used to create additional features for an automated procedure adapting the DLM to the height data. It is the specific goal of this paper to present a new method for matching the borderlines of rivers to the ALS data. Rivers typically have an accuracy of 3-5 m in the ATKIS DLM, with local deviations that may reach 10 m. The ALS point cloud we use has an accuracy of approximately 0.3 m in the horizontal position and 0.15 m in height, so that a considerable improvement should be achievable. To increase the accuracy of river borderlines using ALS data, features extracted in the DSM could be matched with DLM objects. In this paper, a top-down method based on active contours is proposed instead. Whereas the contour is initialized by the vector data, the DSM or related products act as the image energy attracting the contour to salient features. Additionally, object knowledge about the specific appearance of rivers in a DSM is used to formulate constraint energies in order to increase the robustness of the approach.

1.2 Related Work

There has been growing interest in an integration of 2D GIS data and the related height information. A procedure for merging incorporated the 2D geometry of the objects into the DTM structure based on a triangulated irregular network (TIN) (Lenk 2001). However, no inconsistencies between the vector data and the DTM were considered. Koch (2006) improved the TIN-based integration methods by a least squares adjustment using equality and inequality constraints in order to incorporate some semantic properties of the objects. This method, besides being very sensitive to the weights of the observations, does not exploit the implicit information about the vector objects contained in the height data, e.g. structure lines at embankments related to roads or rivers. In (Goepfert & Rottensteiner, 2009) we have done so by adapting active contours to ALS data to improve the positional accuracy of road networks.

Snakes or parametric active contours are a well-known concept for combining feature extraction and geometric object representation (Kass et al., 1988; Blake & Isard, 1998). They explicitly represent a curve with respect to its arc length. In the standard formulation they cannot handle changes in the topology such as splitting and merging of entities (McInerny & Terzopoulos, 1995). This is not a problem for the adaptation of the 2D vector data to ALS features, because the initial topology is taken from the GIS data base and should be held fixed during the process. In the context of river borderlines, the concept of twin snakes introduced by Kerschner (2003) is relevant, because twin snakes connect two approximately parallel lines with a predefined distance. Earlier, Fua (1996) proposed a similar concept called ribbon snakes. Here the width of the ribbon is modelled by an extension of the internal energy and the image energy is calculated at the borderlines of the ribbon. Snakes are widely used in image and point cloud analysis as well as GIS applications. For example, Burghardt and Meier (1997) propose an active contour algorithm for feature displacement in automated map generalisation. Cohen and Cohen (1993) introduce a finite elements method for 3D deformable surface models. Borkowski (2004) shows the capabilities of snakes for break line detection in the context of surface modelling. Laptev et al. (2001) extract roads using a combined scale space and snake strategy. Several papers also deal with the modelling of rivers in height data. Brockmann and Mandlburger (2001) present a technique to extract the boundary between land and river based on bathymetric and ALS data. Fua (1998) simultaneously modelled drainage channels and the surrounding terrain from multiple images using a model-based optimisation scheme in order to express geometric, photometric and physical properties of the object of interest.

2. METHOD

2.1 General Work Flow

In this paper a new method based on an expansion of the twin snakes concept is proposed in order to adapt river borderlines from the ATKIS DLM to ALS data. The image and constraint energies are reformulated so that they represent the specific appearance of rivers in height data while the river borderlines conform to the physical properties of rivers. Whereas the 2D vector data are used for the initialization of the contour (cf. section 2.2), preprocessed ALS height and intensity data define the image energy forcing the snake to salient features (cf. section 2.3). Additionally, object knowledge is introduced in the algorithm (cf. section 2.4) in order to stabilize the optimization process and to obtain a suitable solution. For this purpose the energy functional of the snake is extended by constraint energies derived from three properties of rivers: (1) simple rivers have two approximately parallel borderlines, (2) rivers flow downhill, and (3) the terrain heights increase monotonically from the river banks to the adjacent areas.

After defining and weighting the different terms of internal, image, and constraint energies an iterative optimisation process is started. In the iteration process, the position of the snake is modified. The average change of the position of the contour points in the current iteration can be used to determine the convergence of the algorithm. Afterwards, the new position of the contour should match the corresponding features for the river borderlines in the ALS data. The novelty of the paper consists in the adaptation of the twin snake concept (Kerschner, 2003) to the requirements of our application, in a new

formulation of constraints taking into account the physical properties of rivers (river flow, gradient directions at river embankments), and in a new definition of the image energy of the snakes based on the appearance of rivers in ALS data.

2.2 Snakes

In the initial idea of snakes, introduced by Kass et al. (1988), the position of contours in images is assessed by an energy functional, which consists of three terms:

$$E^*_{snake} = \int_0^1 E_{Snake}(v(s))ds \tag{1}$$
$$= \int_0^1 (E_{int}(v(s)) + E_{image}(v(s)) + E_{con}(v(s)))ds$$

where $v(s) = (x(s), y(s))$ represents the parametric curve with arc length s. The internal energy E_{int} determines the elasticity and rigidity of the curve considering the natural behaviour of the desired objects. The features of the object of interest should be represented in the image energy E_{image} in an optimal way. These features attract the contour to a suitable position. Furthermore, constraints can be defined in additional energy terms (E_{con}), which determine external forces. For example, the contour could be connected to fixed points using spring forces. The internal energy is motivated by the definition of curves forcing the contour to stay smooth linear objects:

$$E_{int}(v(s)) = \frac{\alpha(s)\cdot|v_s(s)|^2 + \beta(s)\cdot|v_{ss}(s)|^2}{2} \tag{2}$$

In Equ. 2, v_s and v_{ss} are the derivatives of v with respect to s, whereas $\alpha(s)$ and $\beta(s)$ are weight functions. The first derivatives, weighted by α, impose a penalty to the arc length of the contour. For that reason, high values of α cause very straight curves. The curvature of the snake is modelled by the second order term, which is controlled by β. Thus, high values of β result in smooth contours, whereas small weights enable a zigzag like behaviour.

If dark or bright lines represent the objects of interest in the images, the image energy (cf. section 2.3) can be simply defined by the grey values. For objects represented by image edges the magnitude of the gradient image may describe this energy term. The global minimum of the energy functional (Equ. 1) determines the optimal position and shape of the snake in the image with respect to the defined energy terms. In order to simplify the optimisation process, the sum of image and constraint energies is replaced by the external energy E_{ext} and the functions α and β are set to constant parameters. After these modifications the minimisation of the functional results in the two independent Euler equations (for x and y):

$$\frac{\delta E_{ext}(v(s))}{\delta v(s)} + \alpha \cdot v_{ss}(s) + \beta \cdot v_{ssss}(s) = 0 \tag{3}$$

Because the derivatives can not be calculated analytically, they have to be approximated by finite differences. With the discrete formulation of the energy functional the weights can be varied easily for each node of the contour. Considering the substitution $f_v(v_i) = \partial E_{ext} / \partial v_i$ with v_i representing the node i the Euler equations can be rewritten:

$$\alpha_i \cdot (v_i - v_{i-1}) - \alpha_{i+1} \cdot (v_{i+1} - v_i)$$
$$+ \beta_{i-1} \cdot (v_{i-2} - 2v_{i-1} + v_i) - \beta_i \cdot (v_{i-1} - 2v_i + v_{i+1}) \tag{4}$$
$$+ \beta_{i+1} \cdot (v_i - 2v_{i+1} + v_{i+2}) + (f_v(v_i)) = 0$$

The matrix form of Equ. 4 reads:

$$Av + f_v(v_i) = 0 \qquad (5)$$

The pentadiagonal banded matrix A in Equ. 5 includes the weights of the internal energy. Equ. 5 is solved by setting the right side equal to the product of a step size γ and the negative time derivatives of the left side. Assuming that the derivatives of the external energy $f_v(v_i)$ are constant during a time step, an explicit Euler step regarding the image energy is obtained. The internal energy completely determined by the banded matrix results in an implicit Euler step if the time derivative is calculated at time t rather than $t-1$. These considerations lead to:

$$Av_t + f_v(v_{t-1}) = -\gamma(v_t - v_{t-1}) \qquad (6)$$

The time derivative vanishes at equilibrium and Equ. 6 degenerates to Equ. 5. The solution is obtained by:

$$v_t = (A + \gamma \cdot I)^{-1} \cdot (\gamma \cdot v_{t-1} - f_v(v_{t-1})) \qquad (7)$$

The following sections describe the derivation of the image energy and the definition of different constraint energy terms.

2.3   Image Energy

Before defining the image energy, we have to discuss what the optimal position of the river borderline in the DTM is. Fig. 1 visualises a cross section of a river bed, the points of interest (black arrows), and the derivatives of the DTM. The points of interest mark the boundary between land and water and correspond to the maximum of the second derivative. The cross section of the intensity data in the vicinity of a river shows a similar structure (Fig. 2a and b). Due to the specular reflection and a high absorption rate in the laser wavelength (1064 nm) water surfaces appear dark in the intensity image. Under certain conditions the reflected echo from water bodies is even too weak to be detected in the receiver device. Therefore, gaps in the scanning pattern can exist. However, very high intensity values can be observed in near-nadir points due to total reflection. This phenomenon does not occur in the analysed data set, but has to be considered in future studies.
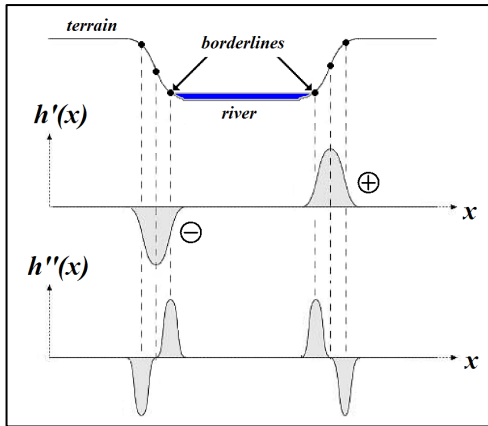

Figure 1.   Cross section of rivers in the DTM

The image energy is generated in three steps. The ALS height and intensity data are first transferred into a regular grid by Kriging (Cressie, 1990). Unfiltered data are used in order to analyse the ability of snakes to bridge disturbances, such as shrubs at river banks in the DSM. The resulting height image I_{DSM} and the intensity image I_{Int} are smoothed by a 3 x 3 median filter to remove outliers while preserving the river edges. In a second step the two images are combined by a weighted sum:

$$I = a \cdot I_{Int} + b \cdot I_{DSM} \qquad (8)$$

In Equ. 8, I is the combined image, and a and b are weights. Analysing the histograms of the images, these weights are set so that the two sources have a similar range of values and thus a comparable influence. The image energy is calculated by the negative magnitude of the second derivatives of the resulting image (Equ. 9). This is realised by convolving the image with the corresponding derivatives of a Gaussian G (Fig. 2c).

$$E_{img} = -\sqrt{\left(\frac{\delta^2 G}{\delta x^2} * I\right)^2 + \left(\frac{\delta^2 G}{\delta y^2} * I\right)^2} \qquad (9)$$

a)   b)   c)
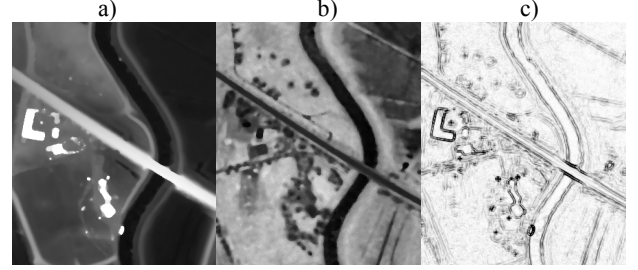

Figure 2. a) DSM b) intensity c) image energy

The boundaries between land and water appear dark in the created image energy, which forces the snake to low grey values. However, other edges in the vicinity of the desired borderline disturb the optimisation process. Therefore, some constraint energies are defined in the next section in order to increase the robustness of the algorithm.

2.4   Constraint Energy

The constraint energy E_{con} is the sum of three components:

$$E_{con} = E_{Twin} + E_{Flow} + E_{Gradient} \qquad (10)$$

The energy E_{Twin} is related to the concept of twin snakes (Kerschner, 2003) and is explained in Section 4.2.1. E_{Flow} is related to the downhill flow direction and is explained in Section 4.2.2. Finally, the term $E_{Gradient}$ takes into consideration the gradient direction of the terrain in the vicinity of the river bank; it is explained in Section 4.2.3.

2.4.1 Twin snakes: Similar to the original constraint energy in Kass et al. (1988), which connects the contour to fixed points by spring forces, Kerschner (2003) developed the idea of twin snakes. In this concept two snakes are linked by a predefined distance d_0. For that purpose the energy functional of each snake is extended by an additional term E_{Twin} that is minimised if the distance of the snakes fulfils the demand:

$$E_{Twin} = \kappa_{Twin} \cdot (d(v_i) - d_0)^2 \qquad (11)$$

In Equ. 11, $d(v_i)$ is the actual distance to the twin at node v_i and κ_{Twin} is the weight of this energy term.

The minimisation of the energy functional is conducted for each contour individually and alternates between the left and right snake. The corresponding other snake is fixed in the meantime. In the optimisation process the derivatives of Equ. 10 with respect to the image coordinates x and y have to be calculated (cf. E_{ext} in Equ. 3) to determine in which direction this energy term moves the contour. The twin energy acts perpendicular to the snake direction either with an attraction or repulsion force. Due to the fact that rivers vary in width a constant value for the predefined distance is not suitable for the proposed application. Assuming a relative quality that is higher than the absolute accuracy of the DLM this distance is derived from the vector

data for each node individually. These values are calculated either as point to point or point to polyline distances. After each iteration the distances are updated. In order to find the inner edges of the bundle of edges along the rivers in the image energy, it is useful to decrease the value for river width from the DLM. A smaller predefined distance increases the attraction force of the two corresponding snakes. The twin energy term supports the delineation of two image edges with a predefined adjustable distance and helps to overcome local minima.

2.4.2   Flow direction: The downhill flow direction of rivers in the DTM is one of the physical properties which are integrated in the algorithm. Due to the effect of the Earth's gravity the nodes in flow direction should show a decreasing or at least a constant height. Initially, a weight $w_{\Delta hi}$ depending on the height differences between the upstream and the downstream nodes h_{i-1} and h_i of one snake is computed:

$$w_{\Delta hi} = \begin{cases} |h_{i-1} - h_i| & if \quad h_{i-1} - h_i < 0 \\ 0 & else \end{cases} \tag{12}$$

Introducing $h(v_i)$ for the terrain height for node v_i and a weight parameter κ_{Flow}, the flow energy term is then defined by:

$$E_{Flow} = \kappa_{Flow} \cdot w_{\Delta hi} \cdot h(v_i) \tag{13}$$

In the minimisation process the derivatives of E_{Flow} at the nodes with respect to the image coordinates x and y have to be calculated (cf. E_{ext} in Equ. 3) similar to the strategy used for the image energy. This approach attracts the nodes that do not satisfy the requirements of the flow direction, from surrounding terrain to lower river areas. The height differences in $w_{\Delta hi}$ act as additional weights. The larger the deviation from the flow constraint for two nodes the stronger is the gradient descent force in the DSM for the node in downhill direction. If some nodes of the snake have already been attracted to the river borderline this energy term has the effect to shift the nodes on higher terrain in their vicinity to the lower river area.

2.4.3   Gradient direction: The third energy term in Equ. 10 exploits the fact that rivers usually flow in valleys and thus the terrain heights increase on each side with the distance from the river. Initially, edge pixels in the DSM are calculated by using the Sobel operator with post processing steps (non-maxima-suppression and hysteresis threshold) following the strategy of Canny (1986). Afterwards, the gradient direction of the edge pixels is computed. Fig. 3b visualises an image in the vicinity of a river with grey value coded gradient directions. Due to the use of the unfiltered data vegetated areas disturb the depicted edges.

For the following considerations we assume the directions of the river borderlines from ATKIS to be correct within certain limits. At each node of the snake we define the direction of the cross-section to be perpendicular to the snake direction. We then analyse the gradient orientations within a small rectangular buffer that is aligned with the direction of the cross-section. The gradient orientations are compared to the directions that are expected based on a model of the cross-section similar to the one depicted in Fig. 1. If these directions are close to each other the edges are labelled as positive, otherwise as negative (see the signs in Fig. 1 for the first derivatives $h'(x)$ for the right snake). By analysing the order of the edges in the vicinity of the river the most probable edge for the current node is chosen considering the typical cross sections of the river (cf. Fig. 3b). We search for two edge pixels with opposite directions in correct order concerning the river profile without another edge

pixel in between. Due to the smoothing effect of the internal energy this constraint is already useful, if the predominant number of choices is correct. The related energy term is defined in a similar way as E_{Twin} in Equ. 14. It is minimised if the distance between the current node and the edge is zero:

$$E_{Gradient} = \kappa_{Gradient} \cdot d(v_i) \tag{14}$$

In Equ. 14, $d(v_i)$ is the distance between the node v_i and the chosen edge and $\kappa_{Gradient}$ represents the weight parameter. The comparison of the snake direction and the gradients enables the approach to deal with poor initialisation. The influence of suitable edges depends on the size of the rectangular buffer. The gradient energy shifts the snakes to the correct gradients (first derivatives) close to the desired edges (second derivatives) and thus into the range of influence of the image energy.

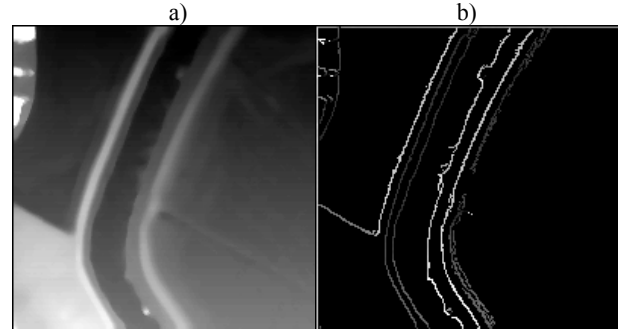a)   b)

Figure 3. a) DSM b) grey value coded gradient direction

3.   EXPERIMENTS

3.1   Data

We use an ALS data set captured near the village Kellinghusen by TopScan during a countywide flight campaign of Schleswig-Holstein between 2005 and 2007. Flying at an altitude of 1000 m the system ALTM 3100 from Optech was used in the first and last echo mode to provide an overall point density of 3-4 points/m^2 and an accuracy of 0.15 m (height) and 0.3 m (position). From the ALS data a 1 m grid is interpolated. The ATKIS vector data set (river borderlines only) was manually manipulated in order to create different initialisation scenarios.

3.2   Effects of the Constraint Energy Terms

The first four experiments emphasise the advantages of the constraint energies in certain conditions. For that reason a higher weight is assigned to the constraint currently considered. The example in Fig. 4a visualises the behaviour of the original snake without constraints. If the initialisation is situated close to the desired edge (upper part of the left snake), the snake moves to the river borderlines. However, with a poor initialisation either the influence range of the image energy is too small to attract the contour (lower part of the left snake) or other edges along the river disturb the final position of the snake (right snake). We want to tackle these problems by integrating the three constraint energy terms. In Fig. 4b the advantages of the twin energy are highlighted. The distance of the initial borderlines is too large, but the approximate river width is known. This information is exploited by the twin energy term. In this case the two snakes are attracted by this part of the energy functional until the range of influence of the image energy is reached. Using actual ATKIS data the assumption is made that the river width is nearly correct and can be used as the predefined distance between the two snakes. With the twin

energy the two contours support each other on their way to a suitable result. Fig. 4c emphasises the effect of the integration of the flow direction in the method. If some parts of the snake have already reached the river borderline, the other nodes in the vicinity are attracted by this force from the surrounding terrain to the lower river region. Due to the high weight for this energy in Fig. 4c and the disturbance caused by shrubs, which hide the true river borderline in the DSM, the nodes in the middle of the right snake move to the centre of the river. The vegetation hampers the fulfilment of the flow direction constraint. Using the gradient direction information (Fig. 4d) helps to deal with poor initialisation. The snakes are able to jump across several wrong edges in the image energy. This additional energy extends the range of the influence of the suitable edges similar to approaches modifying the image energy based on a distance transformation (gradient vector flow by Xu & Prince, 1997).
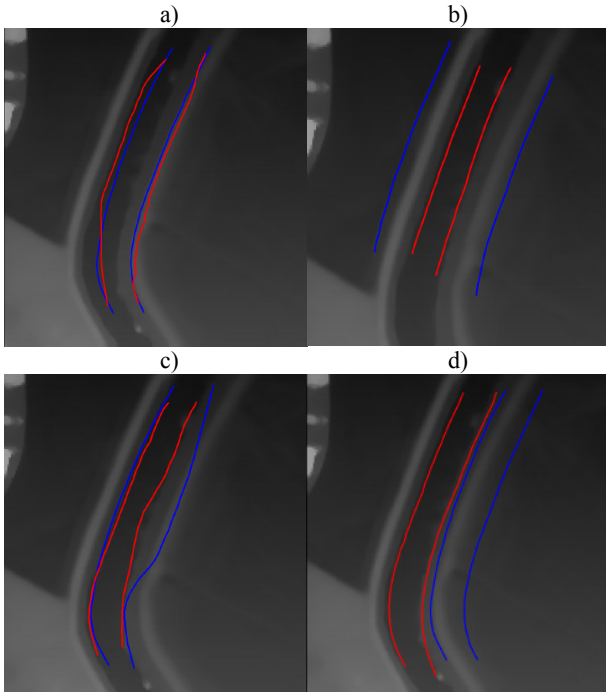

Figure 4. Initialisation scenarios for the different constraints (blue: initialisation; red: final solution): a) without constraints; b) twin snakes c) flow direction; d) gradient direction.

	α	β	κ_{Image}	κ_{Twin}	κ_{Flow}	$\kappa_{Gradient}$
Figure 5	0.16	1.2	3	0.2	10	0.05

Table 1: Weights for the energy terms used for Fig. 5 and 6.

3.3 Results and Discussion

Fig. 5 depicts the adaptation of river borderlines with different initialisations to show the robustness of the method. The empirical weights for the different energy terms of all following examples are shown in Table 1. The algorithm can adapt the 2D vector data, systematically shifted in x-direction by 10 m (Fig. 5a) and 15 m, to the ALS information. Even vegetation and the bridge in the middle of the image do not significantly influence the result. However, if the vector data are shifted by 20 m (Fig. 5b) some parts of the snakes do not reach the correct position any more. These problems (yellow arrows) occur at both ends of the snakes, in areas of strong curvature, and in the vicinity of vegetation and the bridge, where the lack of suitable image energy affects the outcome of the algorithm. For evaluation purposes the root mean square (RMS) values of the

perpendicular distances of the nodes to the reference are calculated (Table 2). In case of 10 m and 15 m shift the errors are smaller than 1.5 m for the left snake and 3 m for the right snake. The poorer result of the right snake is caused by the systematic shift of the initialisation. The entire right snake has to cross the river embankments with several edges in order to move to the correct position. The constraint energy terms attenuate while approaching the desired edge and the snake is sometimes caught in a local minimum related to another edge from the river borderline. Therefore, it is assumed that the algorithm is able to solve random errors of the ATKIS data significantly better, which sometimes cross the correct position.
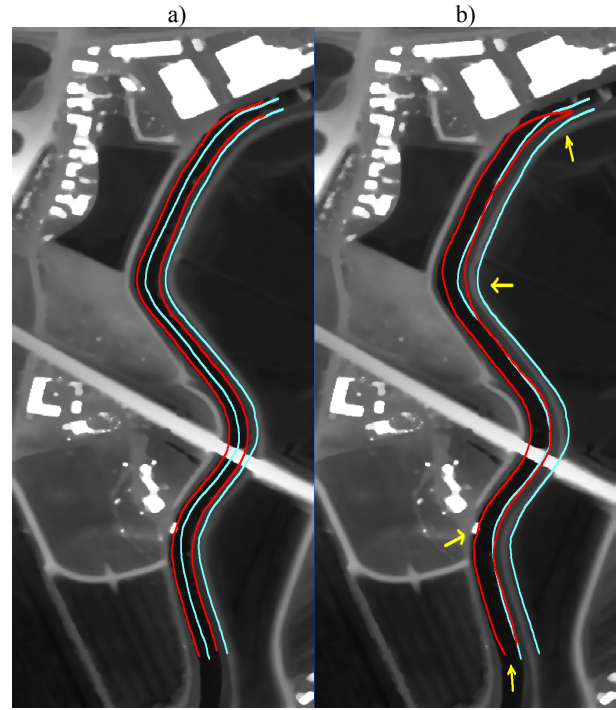

Figure 5. Adapted river with different initialisation (light blue: initialisation; red: final solution) a) x-shift: 10 m b) x-shift: 20 m

RMS of point to line distances (m)	shift: 10 m		shift: 15 m		shift: 20 m	
	left	right	left	right	left	right
Initialisation	8.90	8.95	13.34	13.42	17.77	17.88
Solution	1.15	2.48	1.23	2.67	3.40	3.31

Table 2: Evaluation of the results in Fig. 5 (left snake: 124 nodes; right snake: 120 nodes)

The method was applied to a second example without changing the parameter settings (Fig. 6 and Table 3). The DSM is strongly influenced by vegetation (Fig. 6a). Tree branches hanging across the river generate strong edges in the image energy (yellow arrows). Without adapting the parameters of the snake the constraint energy terms are not able to release the upper snake from the related minima. By using filtered ALS data the snakes move to a suitable solution comparable to the first example without changing the parameters (Fig. 6b). However, once more the systematic shift affects the snake in the shift direction (in this example the lower snake) more than the other. In summary, the accuracy achieved is not entirely satisfying yet for the snake that is initialised to be furthest away from the river. However, difficulties in fixing a suitable reference position, which is done manually, and the resolution of the used grids of 1 m have to be considered in this context.

RMS of point to line distances (m)	DSM		DTM	
	upper	lower	upper	lower
Initialisation	8.16	8.13	8.16	8.13
Solution	3.01	2.53	1,04	2.42

Table 3: Evaluation of the results in Fig. 6 (upper snake: 101 nodes; lower snake: 104 nodes)
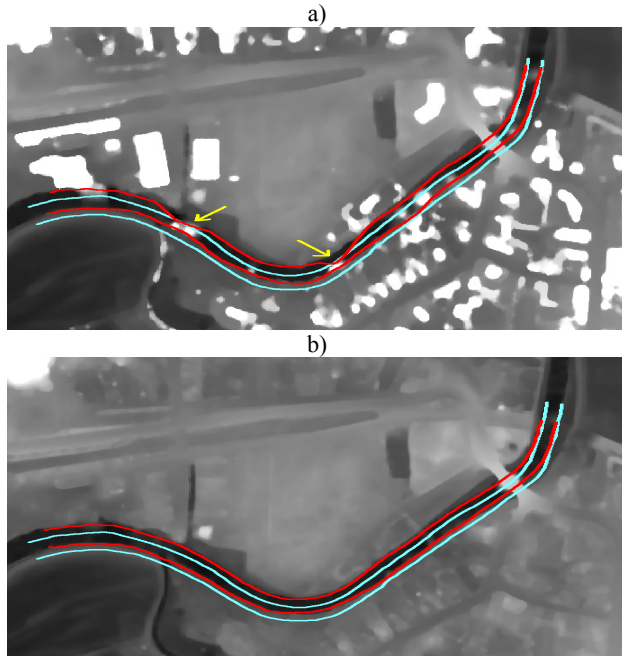
a)

b)

Figure 6. Adapted river with 10 m y-shift using unfiltered (a) and filtered (b) ALS data (light blue: initialisation; red: final solution)

4. CONCLUSION

This paper is focused on a method for adapting river borderlines to ALS features by means of active contour. For that purpose the snake algorithm is extended by three constraint energy terms derived from object knowledge. The connection of the two river sides in the twin energy, and the information about the flow direction as well as the gradient direction at the river banks stabilise the robustness of the basic active contour algorithm and enable the method to deal with poor initialisations. In future work a combination of the proposed constraints and the topology of larger river networks will be integrated in the concept. This algorithm is only one step to a larger framework which we develop in order to solve the inconsistencies between the DLM and height information. All objects in the vector data, which are represented by suitable features in the terrain model, should be adapted. This process provides a dense network of shift vectors which can be used in addition to prior accuracy knowledge in order to improve the consistency of the DLM and ALS data. Furthermore, some objects, such as river and road networks, can be treated together. For example, the bridge in Fig. 5 disturbs the adaptation process of rivers. Bridges are strong feature in the terrain model which can be used to connect rivers and roads in a combined optimisation.

ACKNOWLEDGEMENT

REFERENCES

Blake, A. and Isard, M., 1998. Active contours. *Springer, Berlin Heidelberg New York*, 351 p.

Borkowski, A., 2004. Modellierung von Oberflächen mit Diskontinuitäten. *Habilitation*, TU Dresden, Germany, 91p.

Brockmann H., Mandlburger G., 2001. Aufbau eines Digitalen Geländemodells vom Wasserlauf der Grenzoder. *Publikationen der DGPF*, Band 10, pp. 199–208.

Burghardt, D. and Meier, S., 1997. Cartographic displacement using the snake concept. In: Förstner, Plümer (eds.), *Semantic modeling for the acquisition of topographic information from images and maps*, Basel, Birkhäuser Verlag, pp. 59-71.

Canny, J., 1986. A Computational Approach to Edge Detection. *IEEE TPAMI*-8(6): 679-698.

Cohen, L. D. and Cohen, I., 1993. Finite element methods for active contour models and balloons for 2-D and 3-D images, *IEEE TPAMI* 15(11): 1131-1147

Cressie, N. A. C., 1990. The origins of Kriging, *Mathematical Geology* 22: 239-252.

Fua, P., 1996. Model-based optimization: Accurate and consistent site modeling. *IntArchPhRS 31 B 3*:222–223.

Fua, P., 1998. Fast, accurate and consistent modelling of drainage and surrounding terrain. *Int. J. Computer Vision 26(3):*215-234.

Goepfert, J., Rottensteiner, F. 2009. Adaptation of roads to ALS data by means of network snakes: *IntArchPhRS 38-3/W8*:24-29.

Kass, M, Witkin, A, Terzopoulos, D., 1988. Snakes: active contour models. *Int. J. Computer Vision* 1(4):321-331.

Kerschner, M. 2003. Snakes für Aufgaben der digitalen Photogrammetrie und Topographie. Phd Thesis. IPF, Vienna University of Technology.

Koch, A., 2006. Semantische Integration von zweidimensionalen GIS-Daten und Digitalen Geländemodellen. PhD Thesis, University of Hannover, DGK-C 601.

Laptev, I., Mayer, H., Lindeberg, T., Eckstein, W., Steger, C. and Baumgartner, A., 2000. Automatic extraction of roads from aerial images based on scale space and snakes, *Machine Vision and Applications* 12: 23-31.

Lenk, U., 2001. 2.5D-GIS und Geobasisdaten - Integration von Höheninformation und Digitalen Situationsmodellen. PhD Thesis, University of Hannover, DGK-C 546.

McInerney, T. and Terzopoulos, D., 1995. Topologically adaptable snakes. *Proc. ICCV*, pp 840-845.

Xu, C, Prince, J.L., 1997. Gradient Vector Flow: A new external force for snakes, *Proc. IEEE-CVPR*, pp. 66-71.